

Power System Optimization with Uncertainty and AC Power Flow: Analysis of an Iterative Algorithm

Line A. Roald*

Daniel K. Molzahn†

Aldo F. Tobler‡

Abstract—Many power system optimization problems are inherently affected by uncertainty, as it is generally impossible to exactly forecast load or renewable generation. Finding solutions that lead to low-cost, yet secure operation for a range of conditions is an important concern to system operators. This paper considers an iterative algorithm for solving power system optimization problems that include models of uncertainty and AC power flow physics. This algorithm iterates between solving deterministic nonlinear optimization problems with the AC power flow model and updating constraint tightenings that adjust the constraints to facilitate secure operation. Decoupling the uncertainty and the nonlinear optimization steps provides several advantages, such as tractability for large-scale problems and the ability to separately apply state-of-the-art techniques for handling the uncertainty and the nonlinearity. Using numerical examples and theoretical analyses, this paper discusses the benefits and limitations of the iterative algorithm in solving general power system optimization problems. This paper further characterizes the behavior of the iterative algorithm with respect to convergence, optimality, and infeasibility, and suggests several modifications to improve performance.

I. INTRODUCTION

With larger shares of electricity generated by renewable energy, uncertainty about the future state of the system is an increasingly important aspect of power systems operation. Specifically, since forecasts for renewable energy generation tend to be inaccurate, uncertainty affects predictions of both renewable generation at large installations and the net load throughout the system. The uncertainty about the power injections is a challenge for system operators, who need to account for a range of possible operating conditions when assessing and mitigating operational risk. If system operation is not planned appropriately, fluctuations in the power injections can lead to frequent deployment of costly emergency measures and increased risk of blackouts. Developing tools for operational planning that ensure low-cost and secure operation is therefore an important concern to system operators.

Safely accommodating uncertainty and ensuring feasibility for a range of possible real-time operating conditions requires a certain level of conservativeness. Security against uncertainty hence comes at a price. Solving power system optimization

problems using, for example, a robust or chance-constrained approach leads to solutions that have higher costs than the corresponding deterministic problems. The aim of the system operator is therefore to find an operating point that strikes the optimal trade-off between security and operational cost. Formulating and solving optimization problems that attain this optimal trade-off is a very challenging task that involves a number of modeling and computational aspects.

One challenge is in the definition of an appropriate model of the uncertainty and a corresponding security criterion. Many methods represent the impact of uncertainty mainly through the objective function, by, e.g., minimizing the *expected* operating cost. These approaches are typically two- or multi-stage approaches based on samples [1]–[5] or stochastic approximation techniques [6], where adverse impacts of the uncertainty realization are reflected in a higher second-stage cost, due to, e.g., a more expensive generation dispatch or emergency measures such as load shedding. Other methods focus more on limiting constraint violations due to uncertainty, and guarantee real-time feasibility. Examples include robust optimization approaches which secure the system against all uncertainty realizations within a given uncertainty set [7]–[11] as well as chance-constrained formulations which limit either the probability of constraint violations [12]–[20] or the expected risk of constraint violations (i.e., *weighted* chance constraints) [21], [22]. Common to all methods that involve uncertainty is that the quality of the solution depends significantly on how the stochastic optimization is reformulated into a deterministic, tractable problem. In this paper, we focus on robust and chance-constrained approaches that aim to obtain solutions which guarantee feasibility via limiting either the probability or risk of constraint violations.

The quality of the solution is also dependent on the choice of the system model. Most of the literature on power system optimization under uncertainty is based on the linear DC power flow approximation, e.g., [1]–[4], [6], [9], [10], [14], [16]–[18], [21], [22]. Linearity provides significant advantages both in characterizing the impact of uncertainty and in solving the resulting optimization problem. However, the DC power flow results can be inaccurate and do not consider reactive power or voltage constraints, which are of importance in, e.g., transmission grid security assessment or distribution grid applications. To ensure secure system operation, a power system model based on the full AC power flow equations is necessary; however, it also significantly complicates the problem. The non-linearity of the AC power flow equations

*: Los Alamos National Laboratory, Center for Nonlinear Systems, Los Alamos, NM 87544, roald@lanl.gov

†: Argonne National Laboratory, Energy Systems Division, Lemont, IL 60439, dmolzahn@anl.gov.

‡: ETH Zürich, Power Systems Laboratory, Zürich, Switzerland, faldo@student.ethz.ch

Support from the U.S. Department of Energy, Office of Electricity Delivery and Energy Reliability under contract DE-AC02-06CH11357.

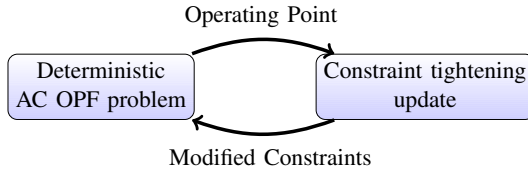


Fig. 1. Conceptual description of the iterative algorithm for solving chance-constrained AC OPF problems.

makes it harder to predict how uncertainty affects power flows and voltage magnitudes throughout the system, and the non-convexity of the corresponding constraints complicates the solution process for the power flow optimization problem. Due to these complications, the literature that considers both uncertainty and AC power flow is very limited. Many existing approaches circumvent these issues by using a linearized version of the AC power flow equations to express the power flow constraints, the impact of uncertainty, or both [12], [13], [19], [20], [23], [24]. Other approaches use a convex relaxation of the AC power flow equations, combined with either a sample-based or analytic chance-constrained representation [15], [25], a two-stage robust optimization method that exploits conic duality [11], or a two-stage stochastic program which uses Benders' decomposition [5]. Due to the high complexity of modelling both AC power flow constraints and uncertainty, many of the above approaches have typically only been demonstrated for small test cases, and scalability to larger systems remains challenging.

In this paper, we investigate an iterative algorithm which allows us to consider the full AC power flow equations and a detailed model of the uncertainty while maintaining computational scalability. The iterative algorithm was first proposed for a Chance-Constrained AC Optimal Power Flow (CC-AC OPF) problem based on a partial linearization in [19]. The algorithm exploits the fact that the chance-constrained problem can be interpreted as a deterministic problem where the constraints have been tightened to accommodate uncertainty. The challenge is to find constraint tightenings that attain an optimal trade-off: large enough to keep the probability of constraint violations below a pre-defined threshold, but as small as possible to avoid unnecessarily high cost. The iterative solution algorithm alternates between solving a deterministic OPF problem and calculating the necessary tightenings associated with the solution point. If the tightenings have changed since the last iteration, the deterministic AC Optimal Power Flow (AC OPF) problem is resolved with the updated tightenings (see Fig. 1). The iterations stop when the tightenings do not change between iterations.

The iterative algorithm decouples the handling of the AC power flow constraints and uncertainty, which is beneficial as it allows us to leverage the robustness and scalability of existing deterministic OPF solvers. The algorithm has been shown to be very efficient for large-scale CC-AC OPF problems [23]. Further, [23] also showed that it is possible to use the iterative algorithm to calculate the tightenings using more detailed representations of the uncertainty and the full, non-linear AC

power flow equations.

In this paper, we analyze and extend the iterative algorithm that was first proposed in [19], [23]. The contributions can be divided into two parts:

Part I. We discuss how the iterative algorithm can be generalized beyond chance-constrained OPF to include other types of power system optimization problems. In particular, we discuss extensions to other chance constraint representations, such as distributionally robust chance constraints and weighted chance constraints, and to problems that include discrete variables, such as unit commitment or transmission switching.

Part II. We investigate the properties of the iterative algorithm with respect to optimality, infeasibility and convergence of the solution. We then suggest modifications to improve the performance of the algorithm.

The paper uses discussions and illustrative numerical examples to emphasize important aspects of the iterative algorithm and the various extensions.

The paper is structured as follows. Section II reviews the iterative algorithm from [19], [23] and summarizes previous discussions on results and benefits of the algorithm. The first main part of the paper, Part I, discusses extensions to the types of problem formulations that the iterative algorithm can capture in its current form. Section III discusses extensions to different types of probabilistic constraints, while Section IV outlines how the algorithm can be used to solve problems that involve integer variables. The second main part, Part II, then considers questions related to optimality of the obtained solution, the impact of infeasibility, and convergence of the algorithm. The section further proposes modifications for improving the algorithm's performance to address these questions. Section V analyzes the performance for continuous problems, while Section VI discusses problems with integer variables. Section VII concludes the paper and summarizes directions for future research.

II. REVIEW OF THE ITERATIVE ALGORITHM FOR CHANCE-CONSTRAINED AC OPTIMAL POWER FLOW

We begin with a brief overview of the iterative algorithm for solving CC-AC OPF problems. We first present the full AC OPF problem with chance constraints and then explain how the problem can be reinterpreted as solving the deterministic version of the problem with tightened constraints. We further describe the iterative algorithm and summarize some observations from previous work. The problem formulation and results presented in this section is a review of results previously presented in [19], [23]. The subsequent sections will present extensions to the iterative algorithm that allow us to handle a broader class of problems.

A. Notation

We consider a power system where \mathcal{N} and \mathcal{L} denote the set of nodes and lines, respectively. The number of nodes and lines are given by $|\mathcal{N}| = m$ and $|\mathcal{L}| = l$. The set of nodes with uncertain demand or production of energy is given by

$\mathcal{U} \subseteq \mathcal{N}$. The set of conventional generators is denoted by $\mathcal{G} \subseteq \mathcal{N}$, and are assumed to be controllable within their limits. To simplify notation, we assume that there is one conventional generator with active and reactive power outputs $p_{G,i}$, $q_{G,i}$, one composite uncertainty source ω , and one demand $p_{D,i}$, $q_{D,i}$ per node, such that $|\mathcal{G}| = |\mathcal{U}| = |\mathcal{N}| = m$. Nodes without generation or load can be handled by setting the respective entries to zero, and nodes with multiple entries can be handled through a summation.

B. Chance-constrained AC optimal power flow

The full CC-AC OPF can be stated as

$$\min_{p_{G,i}, q_{G,i}, v, \theta} \sum_{i \in \mathcal{G}} (c_{2,i} p_{G,i}^2 + c_{1,i} p_{G,i} + c_{0,i}) \quad (1a)$$

$$\text{s.t. } f(\tilde{\theta}(\omega), \tilde{v}(\omega), \tilde{p}(\omega), \tilde{q}(\omega)) = 0, \quad \forall \omega \quad (1b)$$

$$\mathbb{P}(\tilde{p}_{G,i}(\omega) \leq p_{G,i}^{max}) \geq 1 - \epsilon_P, \quad \forall i \in \mathcal{G} \quad (1c)$$

$$\mathbb{P}(\tilde{p}_{G,i}(\omega) \geq p_{G,i}^{min}) \geq 1 - \epsilon_P, \quad \forall i \in \mathcal{G} \quad (1d)$$

$$\mathbb{P}(\tilde{q}_{G,i}(\omega) \leq q_{G,i}^{max}) \geq 1 - \epsilon_Q, \quad \forall i \in \mathcal{G} \quad (1e)$$

$$\mathbb{P}(\tilde{q}_{G,i}(\omega) \geq q_{G,i}^{min}) \geq 1 - \epsilon_Q, \quad \forall i \in \mathcal{G} \quad (1f)$$

$$\mathbb{P}(\tilde{v}_j(\omega) \leq v_j^{max}) \geq 1 - \epsilon_V, \quad \forall j \in \mathcal{N} \quad (1g)$$

$$\mathbb{P}(\tilde{v}_j(\omega) \geq v_j^{min}) \geq 1 - \epsilon_V, \quad \forall j \in \mathcal{N} \quad (1h)$$

$$\mathbb{P}(\tilde{i}_{ij}(\omega) \leq i_{ij}^{max}) \geq 1 - \epsilon_I, \quad \forall ij \in \mathcal{L} \quad (1i)$$

$$\theta_{slack} = 0 \quad (1j)$$

The objective (1a) is to minimize the cost of active power generation, where c_2 , c_1 and c_0 are the quadratic, linear and constant cost coefficients. Eq. (1b) are the nodal power balance constraints based on the full non-linear AC power flow equations. These equations are functions of the nodal voltage magnitudes $\tilde{v}(\omega)$ and angles $\tilde{\theta}(\omega)$ as well as the nodal injections of active power $\tilde{p}(\omega)$ and reactive power $\tilde{q}(\omega)$:

$$\begin{aligned} \tilde{p}_i(\omega) &= \tilde{v}_i(\omega) \sum_{k=1}^n \tilde{v}_k(\omega) \left(\mathbf{G}_{ik} \cos(\tilde{\theta}_i(\omega) - \tilde{\theta}_k(\omega)) \right. \\ &\quad \left. + \mathbf{B}_{ik} \sin(\tilde{\theta}_i(\omega) - \tilde{\theta}_k(\omega)) \right) \end{aligned} \quad (2a)$$

$$\begin{aligned} \tilde{q}_i(\omega) &= \tilde{v}_i(\omega) \sum_{k=1}^n \tilde{v}_k(\omega) \left(\mathbf{G}_{ik} \sin(\tilde{\theta}_i(\omega) - \tilde{\theta}_k(\omega)) \right. \\ &\quad \left. - \mathbf{B}_{ik} \cos(\tilde{\theta}_i(\omega) - \tilde{\theta}_k(\omega)) \right) \end{aligned} \quad (2b)$$

where \mathbf{G} and \mathbf{B} denote the real and imaginary components, respectively, of the network admittance matrix. The power injections are $\tilde{p}_i = \tilde{p}_{G,i}(\omega) + p_{D,i}$ and $\tilde{q}_i = \tilde{q}_{G,i}(\omega) + q_{D,i}$, where $p_{D,i}$ and $q_{D,i}$ are the active and reactive demand at bus i . Note that the power injections and voltages vary with the realization of the uncertain injections ω . These changes are necessary to maintain power balance, e.g., through automatic generation control (AGC), and the desired voltage profile. These changes are modelled as described in [23].

The remaining equations are generation constraints for active and reactive power (1c)–(1f), constraints on the voltage magnitudes at each bus (1g), (1h), and transmission constraints

in the form of flow limits on the current magnitudes $\tilde{i}(\omega)$ (1i). These constraints are affected by the realization of the uncertainty, and cannot be directly enforced in a similar way as deterministic constraints. Instead, we formulate these constraints as chance constraints with acceptable violation probabilities of ϵ_P , ϵ_Q , ϵ_V , and ϵ_I . These chance constraints limit the probability of constraint violations for each constraint separately. Some of the constraints, such as the transmission constraints, are inherently soft constraints that can be violated for a limited period of time without causing problems to the system. If ϵ_I , ϵ_V are chosen sufficiently small, it is unlikely that the constraints will be violated for an extended period of time. Other constraints, such as the generation constraints, are inherently hard constraints, which are physically impossible to violate. For the generation constraints, we interpret the violation probability ϵ_P , ϵ_Q as the probability that the operator will need to take unplanned emergency control actions (e.g. deploy emergency reserves to maintain system balance).

C. Chance-constraint reformulation

The chance constraints given in (1c)–(1i) require reformulation to become tractable. As an example, we review the analytical chance-constraint reformulation proposed in [19], [26], which is based on a linearization of the AC power flow equations around the forecasted operating point.

We use the current flow constraint (1i) for line ij as an example. Denoting the sensitivity factors based on the linearized AC power flow equations as Γ_I and the scheduled operating point by $\mathbf{x} = (p, q, v, \theta)$, we express the chance constraint as the sum between the current flows at the forecasted operating point and approximate changes due to the fluctuations:

$$\mathbb{P}(i_{ij}(\mathbf{x}) + \Gamma_{I(ij,\cdot)}(\mathbf{x}) \omega \leq i_{ij}^{max}) \geq 1 - \epsilon_I, \quad \forall ij \in \mathcal{L}. \quad (3)$$

Note that the sensitivity factor $\Gamma_{I(ij,\cdot)}(\mathbf{x})$ relating the uncertainty ω in the power injections to i_{ij} is a function of the decision variables \mathbf{x} . The exact expressions for $\Gamma_{I(ij,\cdot)}(\mathbf{x})$ can be found in [23].

With the partial linearization, the approximated chance constraint (3) depends linearly on ω . Using this fact and assuming that ω follows a multivariate normal distribution with zero mean and covariance matrix Σ_W , we can reformulate (3) in the following expression:

$$i_{ij}(\mathbf{x}) + \Phi^{-1}(1 - \epsilon_I) \|\Sigma_W^{1/2} \Gamma_{I(ij,\cdot)}(\mathbf{x})^T\|_2 \leq i_{ij}^{max} \quad (4)$$

where $\Phi^{-1}(\cdot)$ represents the inverse cumulative distribution function of the standard normal distribution, $\Sigma_W^{1/2}$ denotes the matrix square root of Σ_W , and $\|\cdot\|_2$ denotes the two-norm. We observe that the chance constraint is equivalent to a tightened version of the deterministic constraint,

$$i_{ij}(\mathbf{x}) \leq i_{ij}^{max} - \lambda_{I,ij}(\mathbf{x}) \quad (5)$$

where the tightening

$$\lambda_{I,ij}(\mathbf{x}) = \Phi^{-1}(1 - \epsilon_I) \|\Sigma_W^{1/2} \Gamma_{I,i}(\mathbf{x})^T\|_2 \quad (6)$$

represents a reduction in the available transmission capacity.

D. Reformulated chance-constrained AC optimal power flow

Performing the analytical reformulation for all chance constraints, we can rewrite the CC-AC OPF problem (1) as

$$\min_{\mathbf{x}} \sum_{i \in \mathcal{G}} (c_{2,i} p_{G,i}^2 + c_{1,i} p_{G,i} + c_{0,i}) \quad (7a)$$

$$\text{s.t. } f(\mathbf{x}) = 0 \quad (7b)$$

$$p_G^{\min} + \lambda_P(\mathbf{x}) \leq p_G \leq p_G^{\max} - \lambda_P(\mathbf{x}) \quad (7c)$$

$$q_G^{\min} + \lambda_Q(\mathbf{x}) \leq q_G \leq q_G^{\max} - \lambda_Q(\mathbf{x}) \quad (7d)$$

$$v^{\min} + \lambda_V(\mathbf{x}) \leq v(\mathbf{x}) \leq v^{\max} - \lambda_V(\mathbf{x}) \quad (7e)$$

$$i(\mathbf{x}) \leq i^{\max} - \lambda_I(\mathbf{x}), \quad (7f)$$

where the tightenings $\lambda_P(\mathbf{x})$, $\lambda_Q(\mathbf{x})$, and $\lambda_V(\mathbf{x})$ have similar expressions as $\lambda_I(\mathbf{x})$ in (6). They also depend on the scheduled operating point, and their exact expressions can be found in [23].

E. Iterative algorithm to solve the chance-constrained AC optimal power flow

Attempting to solve the optimization problem (7) in one shot is possible, but can lead to long convergence times and numerical issues due to the complexity of the expressions for the tightenings $\lambda_P(\mathbf{x})$, $\lambda_Q(\mathbf{x})$, $\lambda_V(\mathbf{x})$, and $\lambda_I(\mathbf{x})$ [23]. One way of circumventing this problem is to solve the problem using an iterative algorithm.

Instead of solving (7) as one combined optimization problem, the iterative algorithm alternates between solving an AC OPF problem (optimizing over \mathbf{x}) corresponding to a fixed vector of tightenings $\hat{\lambda}$,

$$\min_{\mathbf{x}} \quad (1a) \quad (8a)$$

$$\text{s.t. } (7b) \quad (8b)$$

$$p_G^{\min} + \hat{\lambda}_P \leq p_G \leq p_G^{\max} - \hat{\lambda}_P \quad (8c)$$

$$q_G^{\min} + \hat{\lambda}_Q \leq q_G \leq q_G^{\max} - \hat{\lambda}_Q \quad (8d)$$

$$v^{\min} + \hat{\lambda}_V \leq v \leq v^{\max} - \hat{\lambda}_V \quad (8e)$$

$$i(\mathbf{x}) \leq i^{\max} - \hat{\lambda}_I, \quad (8f)$$

and then determining the value of $\hat{\lambda}$ for the corresponding \mathbf{x} ,

$$\hat{\lambda} = \lambda(\mathbf{x}). \quad (9)$$

The algorithm is deemed to have converged when the tightenings have converged (within a specified tolerance η) to fixed values. When this happens, we know that the obtained solution is a feasible solution to the original problem (7). A schematic representation of the iterative algorithm is given in Fig. 2.

F. Benefits of the iterative algorithm

In [23], the iterative algorithm was found to be very effective in solving AC OPF problems. For the considered cases, the iterative algorithm converged to the same solution obtained by a local solver applied to the coupled problem (7), but with lower computational time. Further, when implemented using the interior point solver in the MATPOWER package [27], the iterative algorithm was computationally tractable for large

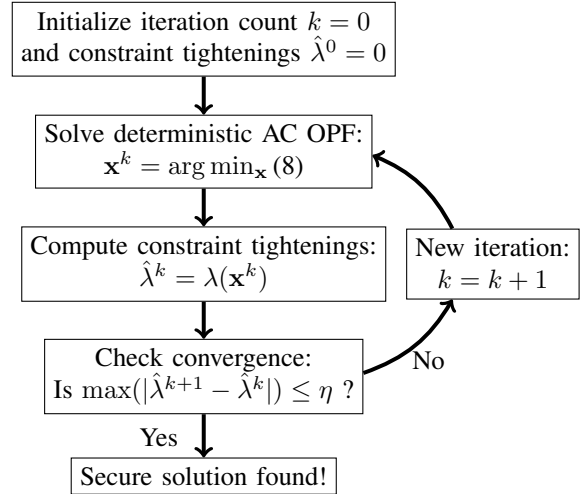


Fig. 2. Iterative algorithm for solving chance-constrained AC OPF problems.

problems (e.g., solving the Polish grid cases with 2383 buses and 941 uncertain loads required less than a minute on a normal desktop computer).

One important characteristic of the iterative algorithm is that it allows us to decouple the tasks of solving the optimization problem and assessing the impact of uncertainty. This decoupling enables the use of more general assessments of the uncertainty's impact such as, e.g., sample-based methods to evaluate the chance-constraints as in [23].

The decoupling through the iterative algorithm further affords the ability to exploit the robustness and scalability of existing and emerging power flow optimization algorithms, and hence leverage decades of progress in solving deterministic AC OPF problems. Since first being formulated by Carpentier in 1962 [28], the solution of deterministic AC OPF problems has been an important research topic. There exist a wide variety of relatively mature solution algorithms for AC OPF problems, including gradient methods, Newton's method, successive quadratic programming, interior point algorithms, etc. [29]–[31]. Many recent efforts have focused on convex relaxation techniques to obtain lower bounds on the optimal objective values and, in some cases, the global optima of AC OPF problems [32]–[37]. Since each iteration only requires the solution of a standard deterministic AC OPF problem, any algorithm from this body of research can be easily extended to consider uncertainty via the iterative algorithm discussed in this paper. For instance, convex relaxation techniques (possibly in combination with local solution algorithms [38]) provide a mechanism for obtaining (at least nearly) globally optimal solutions to the deterministic AC OPF problems (8) despite the presence of, e.g., a disconnected feasible space. Other emerging AC OPF solution techniques, such as algorithms based on penalization methods [39] and continuation methods [40], can also be applied as they mature.

PART I: EXTENSIONS TO MORE GENERAL PROBLEM FORMULATIONS

The benefits described in Section II-F make the iterative algorithm valuable in more general contexts than chance-constrained optimal power flow. Most importantly, the iterative algorithm decouples the optimization and uncertainty assessment, which enables the use of established, more accurate, and computationally intensive techniques for each of the two steps. In particular, the iterative algorithm has the ability to solve a range of other optimization problems involving AC power flow physics. The iterative algorithm further facilitates the use of alternative ways of considering uncertainty beyond chance constraints. The following two sections discuss some generalizations of the iterative algorithm to handle a broader class of problems.

III. EXTENSIONS TO DISTRIBUTIONALLY ROBUST AND WEIGHTED CHANCE CONSTRAINTS

An important benefit of decoupling the optimization and uncertainty assessment is the flexibility to adopt more general definitions of the constraint tightenings without any major change to the overall solution approach. For example, we can apply uncertainty quantification methods with higher accuracy, but also higher computational complexity (e.g., Monte Carlo simulations [23]), or extend the algorithm beyond chance-constraints to a much larger class of problems that address feasibility and risk of operation under uncertainty (such as weighted chance constraints [21]). In this section, we show how the iterative algorithm can be adapted to enforce (1) distributionally robust versions of the chance constraint, (2) a sample-based chance constraint evaluation of the tightenings, and (3) weighted chance constraints which are also evaluated using samples.

A. Distributionally Robust Chance Constraint Evaluation

In many cases, only limited information about the uncertainty distribution is available. To ensure that the violation probability remains below the threshold in this case, we can enforce *distributionally robust* chance constraints which hold for a family of distributions. There are several ways in which we can robustify our chance constraints against uncertainty about the distribution. In [41], the chance constraints are robustified against uncertain distributional parameters (i.e., the mean μ and the variance Σ of the normal distribution are not exactly known, but fall within a certain range). Refs. [18], [42] assume that while the distributional parameters μ , Σ are known, the distribution itself can be any distribution with the same μ and Σ . In the following, we will enforce the latter kind of distributional robustness, where the ambiguity is related to the type of distribution rather than its parameters.

The distributionally robust chance constraints are implemented using a similar analytical reformulation as in Section II-C, which is based on a linearization around the expected operating point. However, while Section II-C provides an example based on the assumption of a normal distribution, similar *distributionally robust* analytical reformulations only

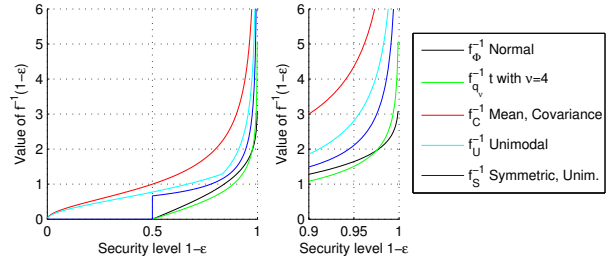


Fig. 3. Values of $f_{\mathcal{P}}^{-1}(1 - \epsilon)$ for the different reformulations [42]. The different lines correspond to the normal distribution (black), the Student t distribution with $\nu = 4$ degrees of freedom (green), symmetric, unimodal distributions (dark blue), unimodal distributions (light blue), and the reformulation based on mean and covariance (red). The left part shows the values for security levels in the range $0 \leq 1 - \epsilon \leq 1$, while the right part shows the values for high security levels $1 - \epsilon \geq 0.9$ in more detail.

assume limited information about the probability distribution. The most general reformulation based on the one-sided version of the Chebyshev inequality only requires information about the mean and variance of the probability distribution,¹ while other reformulations can use additional assumptions such as symmetry or unimodality of the distribution. The examples below are based on the analytical reformulations that were derived and applied to DC power flow in [42].

The general form remains the same as in (6), with the inverse cumulative distribution function $\Phi^{-1}(1 - \epsilon)$ replaced by a more general function $f_{\mathcal{P}}^{-1}(1 - \epsilon)$,

$$\lambda_{I,ij}(\mathbf{x}) + f_{\mathcal{P}}^{-1}(1 - \epsilon_I) \|\Sigma_W^{1/2} \boldsymbol{\Gamma}_{I(ij,\cdot)}(\mathbf{x})^T\|_2 \quad (10)$$

Some possible choices for $f_{\mathcal{P}}^{-1}(1 - \epsilon)$ can be found in Table I. Here, reformulation 1) corresponds to assuming a normal distribution as in Section II-C, while the expressions for 2)-4) correspond to distributionally robust reformulations that hold for all distributions that satisfy certain conditions. Reformulation 2) is valid for all distributions that share the same mean and variance, and in addition are symmetric and unimodal. Reformulation 3) holds for a larger group of distributions as it does not require symmetry (but still assumes unimodality). Reformulation 4) is the most general, as it holds for all distributions that share the same mean and variance. The value of $f_{\mathcal{P}}^{-1}(1 - \epsilon)$ for different values of $(1 - \epsilon)$ is plotted in Fig. 3.² Note that the reformulations which guarantee the chance constraint with less knowledge (i.e., more distributionally robust) have larger values for $f_{\mathcal{P}}^{-1}(1 - \epsilon)$, indicating that a larger tightening is required to limit the violation probability. A more thorough discussion of the different reformulations and a derivation of the expressions for $f_{\mathcal{P}}^{-1}(1 - \epsilon)$ can be found in [42].

¹Note that the probability distribution here refers to the output distributions, i.e., the distribution of the generator outputs, current flows or voltage magnitudes, and not to the input distribution, i.e., the distribution of ω .

²The figure also includes the tightenings corresponding to a Student t distribution, which provides additional security compared with the normal distribution for small violation probabilities ϵ and can be used to model heavy-tailed distribution.

TABLE I
EXPRESSIONS FOR $f_{\mathcal{P}}^{-1}(1 - \epsilon)$ [42].

1) Normal	$f_{\Phi}^{-1}(1 - \epsilon) = \Phi^{-1}(1 - \epsilon)$ Φ : CDF of the standard normal distribution
2) Symmetry, Unimodality	$f_S^{-1}(1 - \epsilon) = \begin{cases} \sqrt{\frac{2}{9\epsilon}} & \text{for } 0 \leq \epsilon \leq \frac{1}{6} \\ \sqrt{3}(1 - 2\epsilon) & \text{for } \frac{1}{6} < \epsilon < \frac{1}{2} \\ 0 & \text{for } \frac{1}{2} \leq \epsilon \leq 1 \end{cases}$
3) Unimodality	$f_U^{-1}(1 - \epsilon) = \begin{cases} \sqrt{\frac{4}{9\epsilon} - 1} & \text{for } 0 \leq \epsilon \leq \frac{1}{6} \\ \sqrt{\frac{3(1-\epsilon)}{1+3\epsilon}} & \text{for } \frac{1}{6} < \epsilon \leq 1 \end{cases}$
4) Mean, Variance	$f_C^{-1}(1 - \epsilon) = \sqrt{\frac{1-\epsilon}{\epsilon}}$ for $0 \leq \epsilon \leq 1$

B. Sample-Based Chance Constraint Evaluation

Since the calculation of the tightenings happens outside of the optimization problem, closed form expressions for the constraints are not required and we need to evaluate them less often. This opens the possibility of defining the tightenings using more computationally burdensome, yet possibly more accurate methods such as Monte Carlo simulations. The section below summarizes the sample-based evaluation approach proposed in [23].

The chance constraint tightening can be understood as an *uncertainty margin*, i.e., a security margin against uncertainty, which allows the constrained value (e.g., current magnitude) to change within some range without violating the defined limit. For any given choice of ϵ , the corresponding uncertainty margin can be understood as the difference between the forecasted value and the $(1 - \epsilon)$ quantile of the distribution.³ While the analytical reformulation determines the necessary uncertainty margin using closed form expressions, the Monte Carlo simulation defines the tightening by constructing the empirical distribution based on samples and empirically evaluating the $(1 - \epsilon)$ quantiles.

To illustrate the calculation of Monte Carlo-based tightenings, we use the current magnitude constraint (5) as an example. A Monte Carlo simulation based on a large number of samples for the uncertainty distribution is used to construct the empirical distribution function of the current magnitude around the forecasted solution $i_{ij}(\mathbf{x})$. Based on the empirical distribution, we determine the $(1 - \epsilon)$ quantile, denoted by $i_{ij}^{1-\epsilon}$. The required constraint tightening is then

$$\hat{\lambda}_{I,ij}^U = i_{ij}^{1-\epsilon} - i_{ij}(\mathbf{x}). \quad (11)$$

Note that the Monte Carlo approach requires neither a linearization around the expected operating point, nor any particular assumption about the underlying probability

³If the forecasted value is sufficiently far away from the actual limit, there will be a small probability of constraint violation. More specifically, if the $(1 - \epsilon)$ quantile is at the limit, there will be exactly ϵ probability that the limit will be violated.

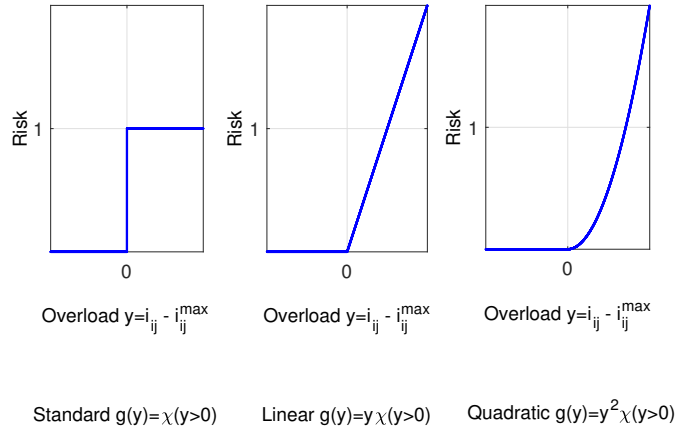


Fig. 4. Example severity functions for the weighted chance constraint [21]. The step function (left) corresponds to a standard chance constraint. The linear weight function (middle) evaluates the expected overload, whereas the quadratic weight function (right) reflects a situation in which large violations incur a higher penalization than small violations.

distribution. This makes it a potentially more accurate approach than the analytical reformulation, although the accuracy depends on the availability of a large number of representative samples, particularly for small violation probabilities.

C. Weighted Chance Constraints

In addition to different methods for determining the constraint tightenings, the iterative algorithm also allows for different formulations of the chance constraints themselves. In many cases, not only the probability of constraint violation but also the magnitude of the constraint violation influences operational risk. One possibility to limit the constraint violation magnitude is by enforcing so-called *weighted chance constraints*, which limit the expected severity (or risk) of constraint overload [21]. Different weight functions can be defined based on how the operator prefers to model risk, with some examples given in Fig. 4. The step function $\chi(y)$, given by

$$\chi(y) = \begin{cases} 0 & \text{for } y \leq 0 \\ 1 & \text{for } y > 0 \end{cases}, \quad (12)$$

corresponds to the standard chance constraint. Choosing an increasing weight function, such as a linear or quadratic function, allows us to assign a higher risk to larger deviations.⁴

As an example, we show how to compute tightenings that correspond to a weighted chance constraint on the current

⁴The linear and quadratic severity functions are also convex, which makes it easier to maintain convexity of the constraints. This property has been used in [21], [22] to model advanced recourse policies and devise efficient solution schemes for problems based on the DC power flow model. For AC power flow, the constraints will in any case be non-convex due to the non-convex power flow equations, so convexity of the weight function might be less of a concern.

magnitude. We will assume a linearly increasing weight function,

$$f(i_{ij}(\mathbf{x}, \omega)) = (i_{ij}(\mathbf{x}, \omega) - i_{ij}^{max})\chi(i_{ij}(\mathbf{x}, \omega) \geq i_{ij}^{max}), \quad (13)$$

where $\chi(y)$ again represents the step function. The linear weight function essentially imposes a limit on the expected overload magnitude [22]. The weighted chance constraint is given by

$$\begin{aligned} & \int_{-\infty}^{\infty} f(i_{ij}(\mathbf{x}, \omega))P(\omega)d\omega = \\ & \int_{-\infty}^{\infty} (i_{ij}(\mathbf{x}, \omega) - i_{ij}^{max})\chi(i_{ij}(\mathbf{x}, \omega) \geq i_{ij}^{max})P(\omega)d\omega \leq \rho, \end{aligned} \quad (14)$$

where $P(\omega)$ is the joint probability distribution of the random variables ω . The parameter ρ corresponds to the risk limit (i.e., the limit on the expected overload), and is given in the same units as i_{ij} [kA].

Similar to the chance constraints, it is possible to evaluate the weighted chance constraints using either a linearization around the expected operating point and the expressions from [21] (originally derived for DC power flow), or using samples. In this paper, we propose to use a sample-based method since the weighted chance constraint requires the evaluation of the integral in (14). This integral depends on the actual values in the tail of the distribution, which makes the evaluation of weighted chance constraints sensitive to linearization errors and incorrect assumptions about the distribution. This is different from the standard chance constraint, which only counts the number of violations and disregards the magnitude.

We evaluate (14) using a Monte Carlo simulation, where we calculate $i_{ij}(\mathbf{x}, \omega)$ for N samples of the uncertain realizations. For each sample m , we calculate the (empirically observed) expected severity $\hat{\rho}^m$ of loading larger than i_{ij}^m . Note that we do not consider the actual limit i_{ij}^{max} in the calculation of the tightenings. Instead, we are looking for the current value i_{ij}^m (belonging to the sample m) above which we would observe $\hat{\rho}^m = \rho$. The difference between this value i_{ij}^m and the forecasted value $i_{ij}(\mathbf{x})$ is then defined as the tightening.

The empirically observed overload for each sample is computed by evaluating the following relation

$$\hat{\rho}^m = \frac{1}{N} \sum_{k=1}^N (i_{ij}^k - i_{ij}^m)\chi(i_{ij}^k \geq i_{ij}^{max}), \quad (15)$$

where the step function $\chi(i_{ij}^k \geq i_{ij}^m)$ ensures that only samples with current magnitudes larger than i_{ij}^m contribute to the risk $\hat{\rho}^m$. After the evaluation, we identify the sample where the empirical overload $\hat{\rho}^m$ is closest to the acceptable expected overload ρ , i.e. where $\hat{\rho}^m = \rho$. The tightening is then defined as the difference between the expected current $i_{ij}(\mathbf{x})$ and the current i_{ij}^m for which $\hat{\rho}^m = \rho$,

$$\lambda_{I,ij} = i_{ij}^m - i_{ij}(\mathbf{x}). \quad (16)$$

Similar to the chance constraint tightening based on Monte Carlo simulations, the accuracy of this approach depends on the availability of a large number of representative samples.

D. Comparison of tightening methods

Above, we have defined tightenings corresponding to (i) analytical chance-constraint reformulations both for the normal distribution and for the distributionally robust case, (ii) chance constraint reformulation based on Monte Carlo simulation, and (iii) reformulation of weighted chance constraints based on Monte Carlo simulation. One of the benefits of the iterative algorithm is the ease of modifying the tightening approach in order to assess the impacts on solution cost and security.

In the following, we compare the tightenings as well as the cost and security of the solutions. We use the IEEE RTS96 system, as distributed with MATPOWER [27], as a test case. To model uncertainty, we assume that renewable generation is connected at lower voltage levels, such that the uncertainty is observed as fluctuations in the net load. The variations in load are modeled using independent normal distributions with zero mean and standard deviations $\sigma = 10\%$ of the forecasted load. In addition, the generation limits are increased by a factor of 1.5 compared to the standard IEEE RTS96 case. We enforce the chance constraints with an acceptable violation probability $\epsilon = 0.1$ and a maximum expected overload of $\rho_I = 0.1$ kA for current constraints, $\rho_P = \rho_Q = 0.1$ MVA for active and reactive power constraints and $\rho_V = 0.001$ p.u. for voltage constraints.

Fig. 5 show the calculation of the different tightenings. In the upper part of the plot, we see the tightening based on the analytical reformulation for the normal distribution (in pink), followed by the distributionally robust reformulations (in light, medium, and dark blue). Note that the tightenings get larger as we assume less and less knowledge about the distribution, such that the tightening based only on knowledge of the mean and variance is 2.5 times larger than the one that assumes a normal distribution.

The chance-constraint tightening which was calculated based on the Monte Carlo simulation (in light green) is close to the analytical tightening for the normal distribution. This is as expected, since the samples used in the Monte Carlo simulation were drawn from a normal distribution. The tightening for the weighted chance constraint (in dark green) is not directly comparable to the other tightenings, as it aims to enforce a limit on the expected overload ρ (determined as the average loading within the dark green region) rather than a violation probability. In particular, we observe that the empirical distribution calculated based on the samples has a quite long tail, i.e., there is a relatively large number of samples with high current values, which contribute significantly to the expected overload. For constraints where the empirical distribution is centered closer to the mean, the tightening of the weighted chance constraint might be smaller than the tightening of the standard chance constraint.

In Table II, we list the objective function cost of each optimization problem solution (top), in addition to the maximum violation probability and maximum expected overloads observed among any single constraint for both an in-sample evaluation (middle) and an out-of-sample evaluation (bottom).

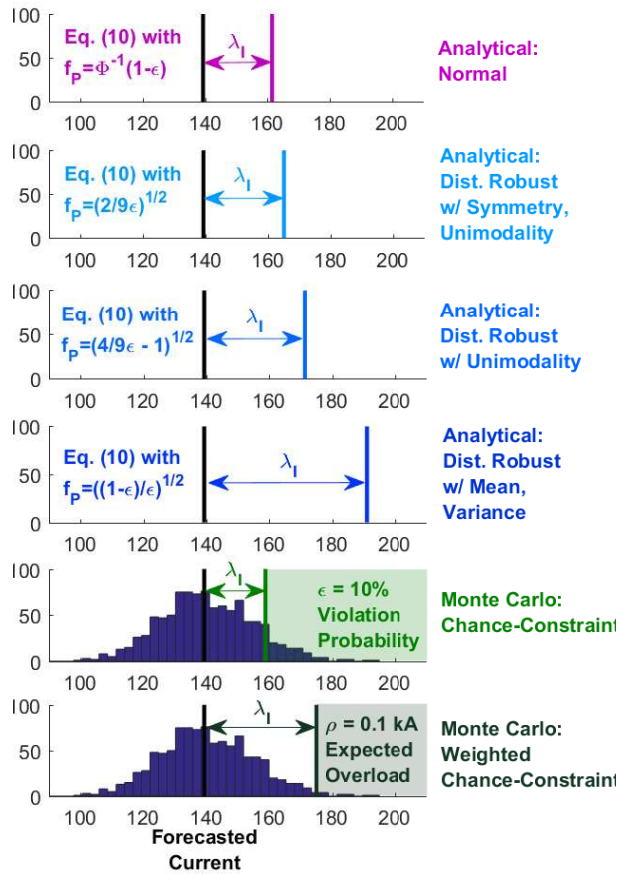


Fig. 5. A conceptual illustration for the computation of the tightenings λ_I for an example current magnitude constraint. The tightenings are derived using the analytical reformulation for a normal distribution (first), and the analytical, distributionally reformulations for symmetric, unimodal distributions (second), unimodal distributions (third), and based only on the mean and covariance (fourth). The two last tightenings are computed based a Monte Carlo simulation and correspond to tightenings that are necessary to enforce a chance constraint (second to last) and the weighted chance constraint (last). For the chance constraints, the acceptable violation probability was $\epsilon = 0.1$ (i.e., 10%), whereas the weighted chance constraint allowed for an expected overload of $\rho = 0.1$ kA.

Note that the out-of-sample evaluation uses a different set of samples for the optimization and evaluation, but still assumes perfect knowledge of the distribution (i.e., the optimization and evaluation samples are drawn from the same multivariate normal distribution).

First, we observe that the costs for the analytical reformulations are increasing as we decrease the knowledge about the distribution (corresponding to an increase in the tightenings). The solution for the normal distribution increases cost by 4.5% relative to the deterministic OPF solution, whereas the distributionally robust solution that only assumes known mean and variance increases cost by 13.1%. The chance constraint reformulation based on the Monte Carlo simulation is the cheapest (+4.4%), while the weighted chance constraint has a slightly higher cost (+6.0%).

Looking at the maximum observed violation probabilities, we observe that the lower-cost solutions lead to higher vio-

lation probabilities (due to the smaller tightenings). This is true for both the in-sample and out-of-sample tests. However, we observe that the tightenings based on the Monte Carlo approach achieves exactly $\epsilon = 0.1$ in the in-sample test, whereas the highest observed violation probability is higher, 0.116, in the out-of-sample test, indicating a sensitivity of the method to the chosen samples. The most frequently violated constraint after the reformulation based on weighted chance constraints is violated in around 50% of the cases. That it is possible to violate the constraint so frequently without violating the expected overload constraint indicates that there are frequent, but very small violations.

This observation is confirmed by looking at the maximum observed overloads. Those overloads are not exceeding $\rho = 0.1$ for the weighted chance constraints in the in-sample test,⁵ while the less-conservative chance constraints (with similar costs) have much larger expected violations. This illustrates the difference between the weighted and standard chance constraints. While the standard chance constraints focus on limiting the frequency of constraint violations, the weighted chance constraints limit the violations' size.

IV. EXTENSIONS TO POWER FLOW OPTIMIZATION PROBLEMS WITH INTEGER VARIABLES

In addition to enabling various types of uncertainty representations, the iterative algorithm could also be extended to other power system optimization problems such as unit commitment, transmission switching, and long-term planning, as well as more general AC OPF problems with detailed device models, such as switched capacitors. Discrete variables are commonly used in these problems to represent such phenomena as on/off state of equipment and investment decisions. Nonlinear problems with integer constraints are particularly challenging to solve [43], and there exists very little literature on how to solve power system optimization problems with discrete variables, uncertainty, and AC power flow constraints. Recently, [5] proposed a two-stage stochastic program to minimize the expected cost of the unit commitment with uncertain wind power injections and a relaxed version of the AC power flow constraints, which was solved using Benders' decomposition. In [24], an adjustable robust formulation for the AC unit commitment with interval uncertainty was solved as a tri-level program. Both of the approaches rely on the use of either a DC power flow or a convex relaxation to solve the problems and have not yet been shown to be applicable to larger systems.

We next discuss how the iterative algorithm can be applied to solve power flow optimization problems with integer variables, using a single-period chance constrained AC unit commitment problem (CC-AC UC) as an example. This problem can be formulated as an AC OPF problem with additional

⁵In the out-of-sample test, the weighted chance constraints experience expected overloads that are 70% higher than prescribed in the worst, which indicates that the computation of weighted chance constraint tightenings are relatively sensitive to the drawn samples.

TABLE II
COST AND OBSERVED VIOLATIONS FOR DIFFERENT REFORMULATIONS.

	Normal Distribution	Analytical Chance-Constraints		Dist. Robust Mean, Variance	Monte Carlo Chance-Constraints	Monte Carlo Weighted Chance-Constraints
		Dist. Robust Symmetry, Unimodality	Dist. Robust Unimodality			
Cost [\$]	38 503	38 819	39 373	41 574	38 404	38 983
(% increase relative to deterministic solution)	(+4.7%)	(+5.6%)	(+7.1%)	(+13.1%)	(+4.4%)	(+6.0%)

TABLE II (A)
IN-SAMPLE TEST OF VIOLATIONS (USING SAME SAMPLES FOR OPTIMIZATION AND EVALUATION)

Max. Violation Probability						
Empirical ϵ [-]	0.111	0.089	0.040	0.006	0.101	0.497
Max. Expected Overload						
Active power [MW]	0.37	0.27	0.10	0.003	0.44	0.10
Reactive power [MVar]	0.52	0.45	0.20	0.02	0.56	0.10
Current [kA]	0.66	0.52	0.14	0	0.85	0.10
Voltage [p.u.]	0	0	0	0	0	0

TABLE II (B)
OUT-OF-SAMPLE TEST OF VIOLATIONS (USING DIFFERENT SAMPLES FOR OPTIMIZATION AND EVALUATION)

Max. Violation Probability						
Empirical ϵ [-]	0.1080	0.080	0.050	0.003	0.116	0.507
Max. Expected Overload						
Active power [MW]	0.33	0.25	0.10	0.00	0.48	0.17
Reactive power [MVar]	0.62	0.41	0.18	0.00	0.38	0.14
Current [kA]	0.70	0.49	0.14	0.00	0.76	0.11
Voltage [p.u.]	0	0	0	0	0	0

binary variables in (17c)–(17f) that allow the generators to be switched off:

$$\min_{p_G, q_G, v, \theta, z} \sum_{i \in \mathcal{G}} (c_{2,i} p_{G,i}^2 + c_{1,i} p_{G,i} + z_i c_{0,i}) \quad (17a)$$

$$\text{s.t. } f(\tilde{\theta}(\omega), \tilde{v}(\omega), \tilde{p}(\omega), \tilde{q}(\omega)) = 0, \quad \forall \omega \quad (17b)$$

$$\mathbb{P}(\tilde{p}_{G,i}(\omega) \leq z_i p_{G,i}^{max}) \geq 1 - z_i \epsilon_P, \quad \forall i \in \mathcal{G} \quad (17c)$$

$$\mathbb{P}(\tilde{p}_{G,i}(\omega) \geq z_i p_{G,i}^{min}) \geq 1 - z_i \epsilon_P, \quad \forall i \in \mathcal{G} \quad (17d)$$

$$\mathbb{P}(\tilde{q}_{G,i}(\omega) \leq z_i q_{G,i}^{max}) \geq 1 - z_i \epsilon_Q, \quad \forall i \in \mathcal{G} \quad (17e)$$

$$\mathbb{P}(\tilde{q}_{G,i}(\omega) \geq z_i q_{G,i}^{min}) \geq 1 - z_i \epsilon_Q, \quad \forall i \in \mathcal{G} \quad (17f)$$

$$\mathbb{P}(\tilde{v}_j(\omega) \leq v_j^{max}) \geq 1 - \epsilon_V, \quad \forall j \in \mathcal{N} \quad (17g)$$

$$\mathbb{P}(\tilde{v}_j(\omega) \geq v_j^{min}) \geq 1 - \epsilon_V, \quad \forall j \in \mathcal{N} \quad (17h)$$

$$\mathbb{P}(\tilde{i}_{ij}(\omega) \leq i_{ij}^{max}) \geq 1 - \epsilon_I, \quad \forall ij \in \mathcal{L} \quad (17i)$$

$$\theta_{slack} = 0 \quad (17j)$$

$$z_i \in \{0, 1\}, \quad \forall i \in \mathcal{G} \quad (17k)$$

The binary decision variable $z_i \in \{0, 1\}$ represents the status of the generator at bus i , and constraints (17c)–(17f) ensure that the power output of a generator is set to zero with probability one when the generator is turned off.⁶ Observe that the objective function (17a) is modified such that generators which are turned off do not contribute to the operating cost.

⁶More general formulations of the unit commitment problem consider multiple time periods, ramp constraints, start-up and shut-down cost, etc. However, the prototypical unit commitment formulation (17) suffices to illustrate the handling of binary variables described in this section.

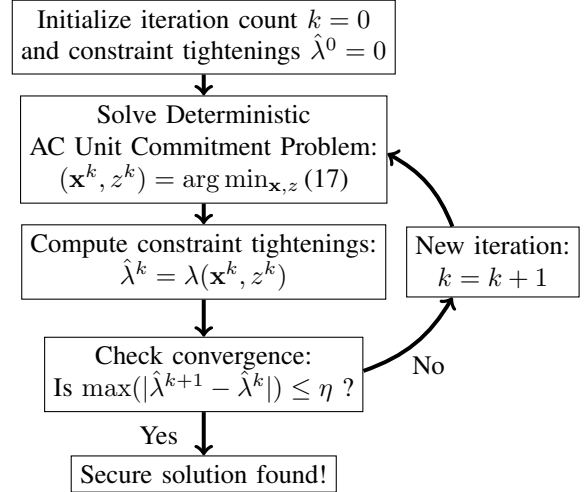


Fig. 6. Conceptual description of the iterative algorithm for solving chance-constrained AC unit commitment problems.

An iterative algorithm analogous to that described in Section II-E for the CC-AC OPF problem (1) is applicable to the CC-AC UC problem (17). In other words, one may replace the deterministic AC OPF problem in Fig. 2 with a deterministic unit commitment problem to obtain an iterative algorithm for solving the CC-AC UC problem. A conceptual representation of this approach is shown in Fig. 6.

While the iterative approach described in Fig. 6 is conceptu-

ally straightforward, the introduction of discrete variables can cause computational problems, as the optimal solution of the deterministic problem can be expected to change more significantly between iterations. The constraint tightenings evaluated at one integer solution might no longer be representative of the tightenings associated with a different integer solution, which could possibly lead to, e.g., convergence problems as discussed in the next section.

PART II: PERFORMANCE ASSESSMENT OF THE ALGORITHM

The iterative algorithm seems to perform well in most practical cases tested so far, and is known to return a secure solution to the stochastic problem (7) in cases where the algorithm converges.⁷ However, we have also observed instances where the algorithm fails to find a solution, and beyond chance-constraint satisfaction, little is known about the quality of the obtained solution. There are several aspects that require a more thorough analysis to appropriately understand the behavior of the algorithm:

- A. *Optimality*: If the algorithm converges, is the result a (locally) optimal solution? Could there be other, lower-cost solutions to the problem that we do not discover?
- B. *Infeasibility*: What does it mean if the optimization problem is infeasible at some iteration in the algorithm?
- C. *Convergence*: Under which conditions does the iterative algorithm converge or fail to converge? Can we modify the algorithm to handle the non-convergent cases?

The following sections discusses each of these points based on empirical studies and theoretical considerations. In thees first part, we analyze the iterative algorithm as applied to continous optimization problems, whereas the second part summarizes our current experiments on problems which also include integer variables. Note that while the numerical examples are currently based on the linearized, analytical chance constraints described in Section II, important characteristics such as the non-convergence phenomenon described below are attributed primarily to the geometry of the feasible region. Other approaches that can be interpreted in terms of a constraint tightening (e.g., the sample-based evaluation of the chance constraints and weighted chance constraints mentioned in Section III-A) can be expected to perform similarly. Thus, the following analysis and suggested modifications are applicable to the iterative algorithm in the context of many problem formulations.

V. PERFORMANCE ASSESSMENT FOR PROBLEMS WITH CONTINUOUS VARIABLES

A. Optimality of the solution

The solution obtained with the iterative algorithm is guaranteed to provide a feasible solution to the original problem when the algorithm converges. As described in Section II-E, the

⁷The security of the solution is defined by the method that is used to compute the tightenings, whether that is a violation probability of a chance constraint or an expected overload.

algorithm is declared to have converged once the tightenings (6) no longer change across iterations and have reached a fixed point $\hat{\lambda}^*$. By design, the solution to the OPF corresponding to this fixed point satisfies

$$\mathbf{x}^* = \arg \min_{\mathbf{x}} (8) \quad \text{and} \quad (18a)$$

$$\hat{\lambda}^* = \lambda(\mathbf{x}^*). \quad (18b)$$

which is a feasible point of the original problem.

In addition to feasibility, optimality of the solution is also an important concern. In previous work [23], the algorithm has been found to converge to a solution which corresponds to the locally optimal solution⁸ found by solving the full problem (7). The aim of this section is to analyze how reliably the algorithm converges to such a locally optimal solution and whether there are any theoretical guarantees for optimality of the algorithm.

One way to assess the robustness of the algorithm's convergence is to check whether it finds the same solution when the tightenings are initialized to different values. To test how sensitive the algorithm is to different starting points, we run several CC-AC OPFs with different initializations of the tightenings. The different initializations are obtained by randomly perturbing the load profile, running the CC-AC OPF with tightenings initialized to zero, and recording the resulting tightening values. The load perturbations were created by drawing uniform random numbers in the range from $\pm 100\%$ of the initial load.⁹ The resulting tightenings were then used as initializations for the CC-AC OPF with the base case load profile. In Fig. 7, we show the results obtained for the IEEE RTS96 case described in Section III-D. We observe that the initial tightenings are quite different, which leads to different costs and different changes in the tightenings in the first iteration. Despite the initial differences, the results rapidly converge to similar tightenings and similar costs. All final solutions have the same cost.

These results indicate that the algorithm reliably converges to the same solution despite differences in the initialization. Although results are shown only for the IEEE RTS96 case, similar observations were made for the IEEE 118-bus and IEEE 300-bus test cases (as described in [23]), indicating that the algorithm performs well for practical systems.

The good empirical performance of the iterative algorithm in solving CC-AC OPF raises the question of whether there are any theoretical guarantees for convergence to an optimal solution. Since the CC-AC OPF problem is hard to analyze theoretically and computationally due to its non-convexity, we ran simulations consisting of a sequence of randomly created linear programs where the standard linear constraints $A\mathbf{x} \leq b$ are augmented with linear tightenings, i.e.,

$$\min_{\mathbf{x}} c^T \mathbf{x} \quad (19a)$$

$$\text{s.t. } A\mathbf{x} \leq b - T\mathbf{x} \quad (19b)$$

⁸There are no guarantees of global optimality, as the problem is non-convex.

⁹Some of the load perturbations lead to infeasible CC-AC OPF problems, but we still recorded the tightenings that the algorithm produced at the points returned by the solver for the infeasible problems.

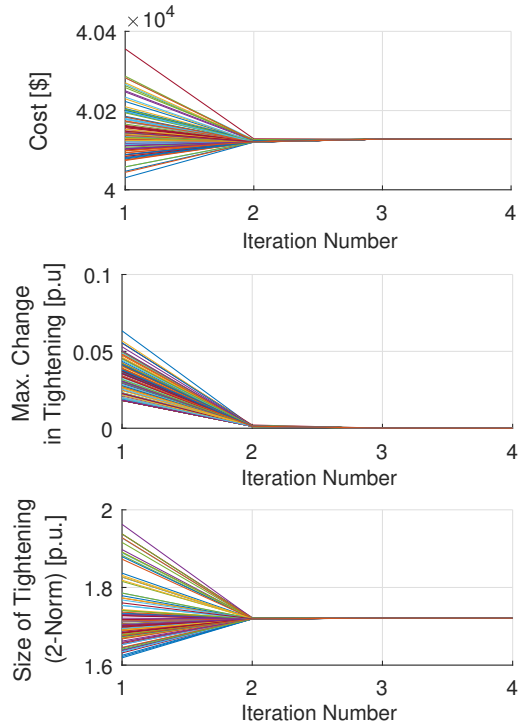


Fig. 7. Convergence of algorithm for different starting points (each line corresponds to a different initialization). The results are for the IEEE RTS96 system, with cost (top), maximum change in tightening between iterations (middle) and the 2-norm of the tightening vector (bottom). The algorithm converges to the same solution in not more than 5 iterations, independent of the initialization of the tightenings.

where the matrix T are the coefficients of the linear function $\tau = T\mathbf{x}$ which defines the constraint tightenings. To obtain different instances, the problem parameters c , A , b , and T were generated at random. For the analysis, we solved the linear program (19) two times, using (1) a standard linear programming solver, which is guaranteed to find the globally optimal solution and can be used as a benchmark, and (2) the iterative algorithm, with tightenings given by $\tau = T\mathbf{x}$ such that we iterate between solving a linear program

$$\min_{\mathbf{x}} c^T \mathbf{x}, \quad \text{s.t.} \quad A\mathbf{x} \leq b - \tau \quad (20a)$$

and evaluating the tightenings

$$\tau = T\mathbf{x}. \quad (20b)$$

Applying iterative solution algorithm to the linear program led to three different outcomes: (i) convergence to the optimal solution, (ii) convergence to a suboptimal solution, and (iii) non-convergence due to cycling (i.e., the algorithm indefinitely repeated a sequence of tightenings). We designed the programs to be feasible, and infeasibility was never encountered in any intermediate iteration. In cases where the tightenings were small (i.e., the magnitudes of the entries τ_i were much less than the magnitudes of the entries in the corresponding row of the A matrix, A_i), the algorithm converged more frequently to the optimal solution. When the tightenings were relatively large, cycling over several iterations and convergence to non-optimal solutions were observed more often.

While the simulations for the randomized linear programs show that the iterative algorithm is not able to reliably solve general optimization problems, the empirical evidence from our current results implies that the algorithm works much better for the CC-AC OPF than for the randomly generated linear programs. There might be several reasons for this. First, the iterative linear problem (20) may have more fixed points than typical non-linear CC-AC OPF problems, leading to more frequent convergence to sub-optimal points. Further, the solution to the linear program is not a continuous function of the problem parameters, as it might jump between different corners of the feasible space, which can induce cycles. Additional analysis and experimentation is required to check if the convergence properties of, e.g., a randomized quadratic program are better.

B. Infeasibility of the stochastic OPF problem

It is plausible that in one of the iterations of the iterative algorithm, the AC OPF is found to be infeasible. If this occurs in the first iteration, where the tightenings are zero, then one can safely conclude that the corresponding CC-AC OPF is also infeasible,¹⁰ since the tightenings $\hat{\lambda}$ are always non-negative. However, AC OPF infeasibility in an intermediate iteration may or may not imply infeasibility of the CC-AC OPF. The tightenings oscillate across iterations, and although one point in the feasible space might have sufficiently large tightenings to make the corresponding deterministic AC OPF infeasible, other feasible points with smaller tightenings might exist.

Even if the algorithm encounters intermediate feasibility in one of the iterations, it is typically possible to evaluate the tightenings for the obtained infeasible point \mathbf{x}^{inf} , particularly if this point is a close to feasible solution of the AC power flow equations. In our experiments, the algorithm was always able to evaluate the tightenings $\lambda(\mathbf{x})$, even for infeasible solutions \mathbf{x}^{inf} . In some cases with such intermediate infeasibility, all subsequent iterations were infeasible, and the algorithm did not converge. However, in many cases, the next iteration did produce feasible OPF solutions, and the algorithm converged. Particularly for the cases where we started with large, non-zero initializations of the tightenings (as in the convergence experiments for the RTS96 system described in Section V-A), the iterative algorithm typically required a few iterations before it reached feasibility, after which it converged to the same solution as the instances which were initialized with tightenings equal to zero.

In the current experiments, we directly used the infeasible point produced by the solver to evaluate the tightenings $\lambda(\mathbf{x}^{inf})$. This infeasible point might or might not be close to a feasible AC OPF solution, depending on the problem and the choice of solver. A more rigorous analysis of the algorithm in case of intermediate infeasibility requires a more precise definition of what it means that the infeasible point is “close” to a feasible solution. One possibility would be to run a second

¹⁰Certifying infeasibility of a deterministic AC OPF problem is NP-Hard [44]; however, convex relaxations can provide sufficient conditions for AC OPF infeasibility [32], [34], [35], [37].

OPF problem where the objective is to minimize the violation of constraints on generator outputs, voltage magnitudes, and line flows while obtaining a feasible solution to the AC power flow equations. In this case, the resulting solution would violate the engineering constraints in the problem but still obey the physics of the AC power flow.

C. Convergence of the algorithm

The iterative algorithm described in Section II has been successfully demonstrated on a range of practical problems. Based on previous experimentation, the algorithm appears to work well for problems where the AC OPF solution does not experience significant, sudden changes between iterations. In this case, the variation in the tightening is typically small, and convergence is reached within a few iterations.

To demonstrate these observations, we run the CC-AC OPF algorithm for the IEEE RTS96, IEEE 118-bus and IEEE 300-bus systems for different violation probabilities ϵ . The resulting number of iterations to convergence and the final cost are shown in Fig. 8. For each system, we observe that the algorithm requires fewer iterations as ϵ increases and the tightening decreases. Furthermore, the final cost is monotonically decreasing as ϵ increases and the tightening is reduced. Note that this smooth reduction in cost indicates that the solutions we obtain are close to each other, with a similar set of active constraints. This once again demonstrates that the algorithm consistently converges to a similar local minimum, instead of converging to very different solutions for each value of ϵ . The cost in Fig. 8 are plotted relative to the deterministic cost. Note that the impact of uncertainty on cost varies between different systems, with the IEEE RTS96 system experiencing the largest relative cost increase. The relative cost increase is indeed case specific, and depends on a combination of the set of active constraints and the size and location of the fluctuations.

However, despite often being successful, the algorithm does not have a convergence guarantee and non-convergence has been observed for some AC OPF test cases. One mechanism for non-convergence is related to the existence of several local optima for the AC OPF problem. In this case, subsequent iterates in the algorithm might cycle between repeated points that have large differences in the associated tightenings. This section illustrates the cycling phenomenon using a small test case, and further describes a “cut-and-branch” modification which interrupts the cycling and results in convergence.

1) Illustrative example of a non-convergent CC-AC OPF test case: A variety of research efforts have investigated the non-convexity of the feasible spaces associated with deterministic power system optimization problems [45]–[49]. The feasible spaces of AC OPF problems can have multiple disconnected regions, each of which contain one or more local optima. The test case described in this section illustrates how these disconnected regions of the feasible space may result in non-convergence of the iterative algorithm.

We consider the five-bus test case in [48] with an uncertain load at bus 4 that has a normal distribution with standard

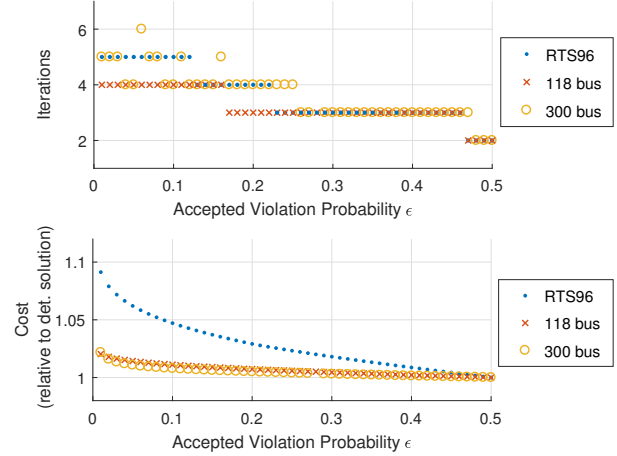


Fig. 8. A comparison of the number of iterations (top) and cost relative to the deterministic solution (bottom) for three different test systems and varying acceptable violation probability ϵ . We observe that the number of iterations decreases as ϵ increases and the tightening becomes smaller. Further, we see that the cost is consistently decreasing as ϵ increases, which suggests that the optimization algorithm converges to a similar local minima.

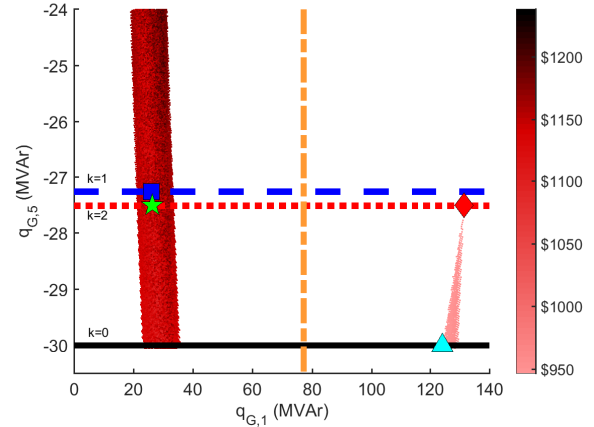


Fig. 9. A projection of the feasible space for the five-bus system from [48]. The colored area represents the feasible space, which has two disconnected regions, and the colors themselves represent the generation cost. The initial deterministic OPF problem has a solution and initial limit $q_{G,5}^{min}$ denoted by the light-blue triangle and the black line. The following iterations have solutions denoted by the blue square and the red diamond with corresponding limits $q_{G,5}^{min} + \hat{\lambda}_{Q,5}^{k=1}$ and $q_{G,5}^{min} + \hat{\lambda}_{Q,5}^{k=2}$ denoted by the blue dashed line and the red dotted line. Each pair of subsequent iterations cycles between points on the left and right sides of the feasible space, resulting in the algorithm failing to converge. The cut-and-branch modification creates two subproblems with feasible spaces that are either to the left or to the right of the vertical orange dashed line. The subproblem to the right is infeasible while the subproblem on the left converges to the green star.

deviation $\sigma = 6\%$. The deterministic problem (i.e., $\hat{\lambda}^0 = 0$ in (8)) has a feasible space with two disconnected components. Fig. 9 shows the projection of (a subset of) the feasible space for the deterministic problem in terms of reactive power generation, computed using the approach in [49]. The OPF problem specifies a lower reactive power limit of -30 MVar for the generator at bus 5 (visualized as the solid black line).

The colors in Fig. 9 show the generation cost. Observe that

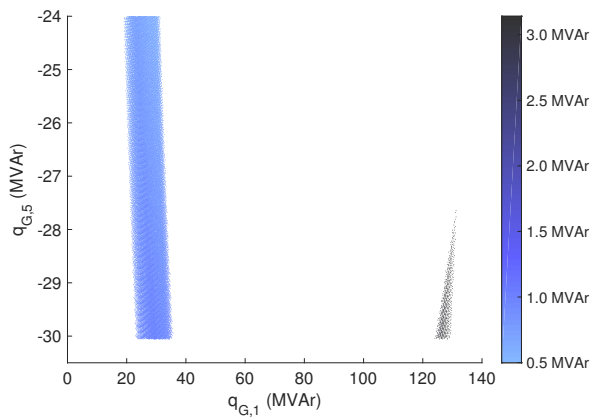


Fig. 10. A projection of the feasible space for the five-bus system from [48]. The colors represent the tightening of the lower reactive power generation limit at bus 5, $\hat{\lambda}_{Q,5}$, computed by the analytic reformulation of the chance constraints as a function of the operating point. The difference in the tightening between the disconnected regions on the left and right sides of the feasible space leads to the cycling phenomenon observed for this test case.

the small region on the right side of Fig. 9 has the lowest cost, so the global solution to the deterministic problem is at the light-blue triangle in this region. Also observe in Fig. 10 that the values for the reactive power tightening $\hat{\lambda}_{Q,5}$ have a non-negligible variation with location in the feasible space.

Using an acceptable violation probability $\epsilon_Q = 0.05$, the second iteration of the algorithm tightens the reactive power limit from -30 MVar to -27.26 MVar, which restricts the feasible space to the region above the blue dashed line and therefore cuts off the region on the right side of Fig. 9. The solution to the OPF problem for this iteration is thus at the blue square on the left side of Fig. 9. The linearization computed at the blue square results in a less-stringent limit of -27.51 MVar for the third iteration. This expands the feasible space to the region above the red dotted line, thus restoring feasibility of the region on the right side of Fig. 9 to yield the solution at the red diamond. The fourth iteration of the algorithm results in a stricter tightening that again eliminates the region of the feasible space on the right side of Fig. 9, returning the OPF solution for this iteration to the region on the left side of the figure. For all subsequent iterations, the algorithm cycles between the same two points, eliminating and restoring the region of the feasible space on the right side of Fig. 9. Thus, the algorithm fails to converge, and neither point in the cycle is a feasible solution to the chance-constrained AC OPF problem.

2) Cut-and-branch modification to avoid cycles and achieve convergence: This section proposes one possible modification which eliminates the cycling phenomenon observed for the five-bus test case, resulting in convergence of the iterative algorithm. Specifically, a “cut-and-branch” modification to the iterative algorithm keeps a history of the tightenings computed

at each iteration.¹¹ If any iteration repeats the tightenings from a previous iteration, indicating the start of a cycle, the modification introduces a constraint that “cuts” the feasible space to create two subproblems in order to interrupt the cycle. While there are many possible cuts, we suggest using the simple approach of adding a constraint on the active or reactive power injection that has the largest difference in value between any pair of points in the cycle. Two subproblems are created by forcing this power injection to be either greater than or less than the midpoint of the distance between the power injections associated with this pair of points. With cycling precluded by this constraint, the iterative algorithm is applied to separately solve each subproblem. This process is potentially repeated to further split the subproblems if cycling is again detected at later iterations.

In the context of the five-bus test case, the cut shown by the vertical orange dashed line creates two subproblems containing the regions on either the left or the right side of Fig. 9. Applying the iterative algorithm to each subproblem results in infeasibility for the subproblem on the right, with the tightening computed at the red diamond cutting off this portion of the feasible space. For the subproblem on the left, the algorithm converges to the solution at the green star.

While this cut-and-branch modification successfully results in convergence for this test case, further work is needed to characterize the convergence behavior of the modified algorithm for other problems. Future research is also required to identify whether there exist other causes of non-convergence and to suggest ameliorating modifications as needed.

VI. PERFORMANCE ASSESSMENT FOR PROBLEMS WITH INTEGER VARIABLES

As discussed in Section IV, it is conceptually straightforward to apply the iterative algorithm to power flow optimization problems with integer variables. The “only” difference is that the algorithm would solve a mixed-integer non-linear program with AC power flow constraints in each iteration instead of a continuous AC OPF.

While the iterative algorithm can be directly applied, there are several reasons to expect differences in performance between the continuous AC OPF problem and related power system optimization problems that include integer variables. Not only are integer optimization problems generally difficult to solve due to the combinatorial nature of the solutions, the integer variables also introduce an increased number of local minima and additional disconnected regions of the feasible space. As opposed to the continuous AC OPF problem, which has been studied in literature for many decades and for which efficient local solvers exist, the literature on deterministic power system optimization problems with both integer variables and AC power flow models is relatively limited. There

¹¹The cut-and-branch algorithm proposed in this paper is similar to “spatial branch-and-bound” techniques used in global optimization solvers (see, e.g., [50]–[52]) in that both separate the feasible space into multiple disjoint regions. However, unlike spatial branch-and-bound algorithms, the iterative algorithm does not attempt to guarantee obtaining a globally optimal solution and therefore does not employ bounding techniques.

are only a few solvers that are applicable to the corresponding non-convex, mixed-integer optimization problems. Integration of the integer variables in the algorithm is hence a practical challenge.

Theoretically, the integer variables make it harder to analyze the solution optimality, as the analysis must now consider large set of integer solutions.¹² Moreover, the integer variables might induce significant changes in the tightenings as the solution jumps from one integer solution to the next, making the iterative algorithm more prone to cycling and less likely to escape intermediate infeasibility.

Due to the relative immaturity of mixed-integer non-convex programming solvers, the iterative algorithm for optimization problems with integer variables problem has not been tested as extensively as the algorithm for the continuous AC OPF problem. However, small test cases are tractable by enumerating each combination of the binary variables to obtain a set of deterministic AC OPF problems, solving these deterministic AC OPF problems, and selecting the solution with minimum objective value.

This section uses the chance-constrained AC unit commitment (CC-AC UC) problems described in Section IV in order to illustrate the convergence characteristics of the iterative algorithm for integer-constrained problems. Application to several small test cases suggests that the iterative algorithm for CC-AC UC problems has similar behavior as for CC-AC OPF problems in that the algorithm tends to converge when the tightenings are relatively consistent across the low-cost region of the feasible space. However, while the iterative algorithm for CC-AC UC problems typically converged for the small test cases considered thus far, existing numerical experiments are too limited to confidently make conclusions on algorithmic performance more generally.

A. Illustrative example of a non-convergent CC-AC UC test case

The five-bus test case discussed in Section V-C1 demonstrates the possibility for non-convergence of the iterative CC-AC OPF algorithm due to cycling behavior. For the five-bus test case, the cycling behavior is associated with multiple local optima for the deterministic AC OPF problem. Despite often converging for small test cases, power system optimization problems with discrete variables, such as unit commitment (UC), can also exhibit similar cycling behavior and thus fail to converge. This will be demonstrated by solving the CC-AC UC (17) for a small test case.

We consider a modified version of the six-bus, three-generator system from [53]. (This test case is known as “case6ww” in MATPOWER [27].) The load and generator parameter values are unchanged. The voltage magnitudes at all buses are constrained to be within 0.95 and 1.10 per unit. Apparent power flow limits of 0.90 per unit are specified for each line. The constant in the cost function for each

¹²Note that it is challenging to obtain rigorous lower and upper bounds for the objective function due to the problem non-convexity.

generator (17a) is $c_{0,i} = 250\$, \forall i \in \mathcal{G}$, with the other cost coefficients remaining unchanged from the values specified in the test case. For this example, the acceptable violation probability is $\epsilon = 0.005$ and the tightenings are computed using the analytic reformulation for a normal distribution, as discussed in Section II-C.

Fig. 12 shows the feasible space of the six-bus system and illustrates the application of the iterative algorithm to the CC-AC UC problem for this test case. The feasible space of the initial iteration is shown in Fig. 12a. The feasible space consists of four disconnected regions, each of which corresponds to a different combination of the generators’ statuses. The initial solution of the deterministic unit commitment problem is at the light-blue triangle in Fig. 12a. The tightenings computed at the light-blue triangle eliminate the regions of the feasible space for which either generator 1 or generator 3 is turned off. The lowest-cost point remaining in the feasible space is at the blue square in Fig. 12b, which is contained in the region with generator 2 off. The tightenings computed at the blue square are such that there exist feasible points for which generator 1 is off. The lowest cost solution with these tightenings is at the red diamond in Fig. 12c. The tightening at this point again eliminates any solution with generator 1 off. All subsequent iterations cycle between the blue square in Fig. 12b and the red diamond in Fig. 12c. Thus, the iterative algorithm fails to converge for this test case. Note that other parameter choices can result in even more complicated cycling behavior, including cycles that include at least four different points.

1) *Cut-and-branch modification to for problems with integer variables:* A similar approach to the “cut-and-branch” modification employed for the CC-AC OPF can be applied to eliminate the cycling behavior. For specified values of the binary decision variables z , observe that the CC-AC UC problem (17) is equivalent to a CC-AC OPF (1) problem. Similar to the cuts in Section V-C2, specifying a combination the generators’ statuses in the CC-AC UC problem can isolate disconnected regions of the feasible space and preclude the cycling behavior. Thus, rather than iterating between solving deterministic AC unit commitment problems and computing constraint tightenings as shown in Fig. 6, an alternate approach for the CC-AC UC problem considers different combinations of the generators’ statuses and solves the CC-AC OPF for this combination. This alternate approach is outlined in Fig. 11.

If the problem is sufficiently small, we are able to solve for each possible combination of the generators’ on/off statuses, and select the lowest-cost solution selected as the overall solution to the CC-AC UC problem.¹³ See Fig. 13 for a conceptual description of the implementation of the alternate approach using the modified six-bus system.

Fig. 14 further illustrates the workings of this alternate algorithm using the feasible space of the six-bus system. Choosing

¹³If needed, the cut-and-branch modification described in Section V-C2 may be used to encourage convergence of the iterative algorithm applied to the continuous CC-AC OPF problems formulated for each combination of the generators’ statuses.

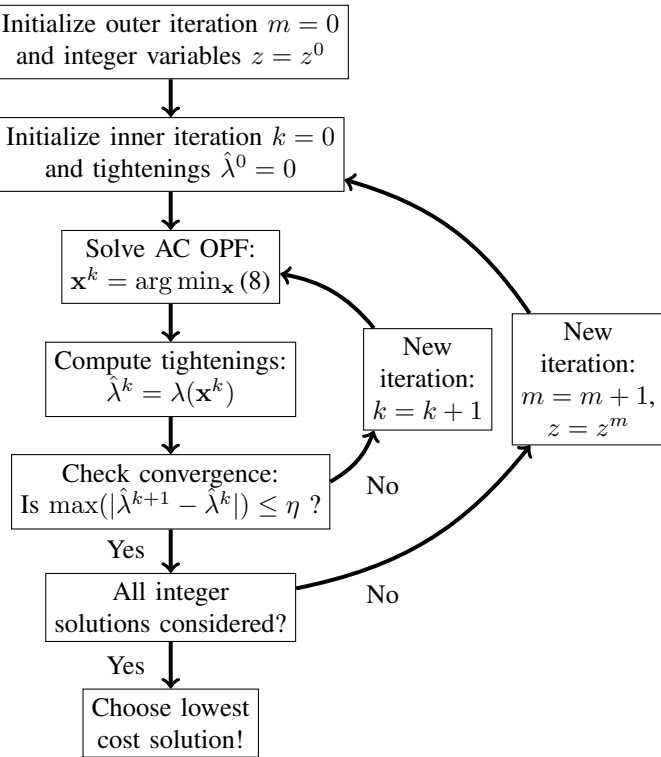


Fig. 11. Conceptual description of the alternate iterative algorithm for solving chance-constrained AC unit commitment problems.

a certain combination of the generators' statuses restricts the feasible space to one of the regions identified by the dashed lines in Fig. 14. The iterative algorithm reports infeasibility for the CC-AC OPF problems corresponding to combinations of the generators' statuses where either generator 1 or generator 3 is turned off. The iterative algorithm converges to the green stars in Fig. 14 for the CC-AC OPF problems corresponding to combinations of the generators' statuses with either all generators are on or only generator 2 turned off. The green star at $[P_{G1} \ P_{G2} \ P_{G3}]^\top = [1.43 \ 0 \ 0.76]^\top$ per unit, which corresponds to the case where generator 1 is off, has lowest cost and is therefore selected as the solution to the CC-AC UC problem.

For the six-bus test case with the alternate approach described in Fig 13, the iterative algorithm for the CC-AC OPF problems either converges or is infeasible for each combination of the generators' statuses. This suggests that the convergence failure when applying the iterative CC-AC UC algorithm in Fig. 6 is a result of the disconnected feasible space created by the binary variables in combination with the relatively large change in tightenings associated with a change in the generators' statuses.

The number of possible combinations of the generators' on/off statuses increases combinatorially with the number of generators. Thus, solving the CC-AC UC problem by exhaustive search over all possible combinations is only computationally tractable for systems with a small number of generators. Defining good heuristics to identify promising integer

solutions and discard others constitutes the most important step towards improving computational tractability of this approach, and is an important subject for future work. One possible direction is to employ a branch-and-bound framework in order to eliminate many possible combinations of the generators' statuses from explicit consideration.

VII. OUTLOOK

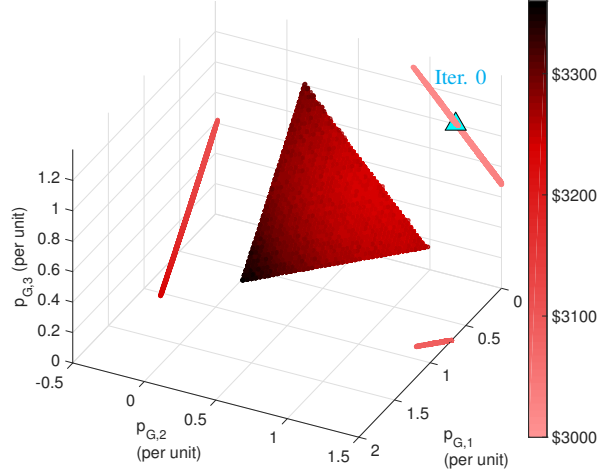
This paper summarizes important aspects of an iterative algorithm for solving power system optimization problems with AC power flow constraints and uncertainty. By decoupling the optimization and the assessment of the uncertainty's impact, the iterative algorithm is able to utilize existing implementations of deterministic power system optimization problems as well as sophisticated tools to characterize the impact of uncertainty. The paper discusses opportunities and limitations with respect to solving general power system optimization problems under uncertainty, including different versions of probabilistic constraints and handling of problems with integer variables. On the other hand, the paper also describes important algorithmic aspects such as convergence to optimal solutions, handling of infeasibility and non-converging cases. The algorithm was found to extend to a large class of power system optimization problems under uncertainty and to perform well in most practical cases. However, the algorithm is not guaranteed to converge to a (local) optimum. Further, it was demonstrated that the existence of several local minima can lead to non-convergence of the algorithm in specific cases. Further investigation is required to fully understand the properties of the algorithm and the quality of the obtained solution.

ACKNOWLEDGEMENTS

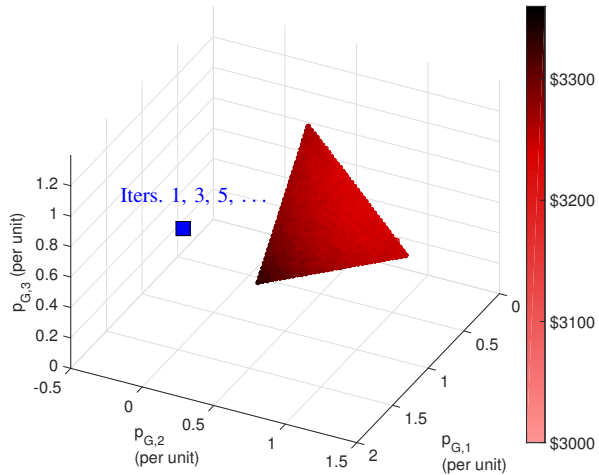
The authors would like to thank Sidhant Misra for multiple discussions and advice regarding the overall paper as well as particular insights related to the analysis of the algorithm's optimality characteristics.

REFERENCES

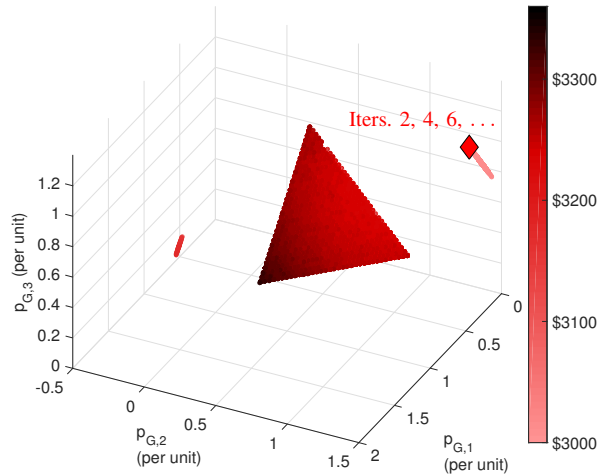
- [1] F. Bouffard and F. D. Galiana, "Stochastic security for operations planning with significant wind power generation," *IEEE Transactions on Power Systems*, vol. 23, pp. 306–316, May 2008.
- [2] J. M. Morales, A. J. Conejo, and J. Perez-Ruiz, "Economic valuation of reserves in power systems with high penetration of wind power," *IEEE Transactions on Power Systems*, vol. 24, no. 2, pp. 900–910, May 2009.
- [3] A. Papavasiliou and S. S. Oren, "Multi-area stochastic unit commitment for high wind penetration in a transmission constrained network," *Operations Research*, vol. 61, no. 3, pp. 578–592, 2013.
- [4] S. C. Müller, V. Liebenau, S. Ruthe, C. Spieker, C. Kittl, S. Dalhues, D. Mayorga, F. Valeri, and C. Rehtanz, "The impact of forecasting errors and remedial actions on operational security and efficiency in classical and probabilistic constrained market coupling," in *Power Systems Computation Conference (PSCC)*, Wroclaw, Poland, Aug. 2014.
- [5] A. Nasri, S. J. Kazempour, A. J. Conejo, and M. Ghandhari, "Network-constrained AC unit commitment under uncertainty: A benders' decomposition approach," *IEEE Transactions on Power Systems*, vol. 31, no. 1, pp. 412–422, Jan 2016.
- [6] T. Tinoco De Rubira and G. Hug, "Adaptive certainty-equivalent approach for optimal generator dispatch under uncertainty," in *European Control Conference (ECC)*, Aalborg, Denmark, 2016.



(a) Iteration 0



(b) Iterations 1, 3, 5, ...



(c) Iterations 2, 4, 6, ...

Fig. 12. A projection of the feasible space for a modified version of the six-bus system from [53]. The colored area represents the feasible space and the colors themselves represent the generation cost. Observe that the feasible space in Fig. 12a has four regions corresponding to the combinations of generator statuses with each generator on and any one of the three generators off. The initial deterministic AC unit commitment problem has a solution shown by the light-blue triangle in Fig. 12a. Each subsequent iteration uses the tightenings computed from the previous iteration, with corresponding (smaller) feasible spaces shown in Figs. 12b and 12c. Iterations 1 and 2 have solutions denoted by the blue square and the red diamond in Fig. 12b and 12c, respectively. The subsequent iterations cycle between the blue square (iterations 3, 5, ...) and red diamond (iterations 4, 6, ...) in Figs. 12b and 12c, resulting in the algorithm failing to converge.

- [7] P. Panciatici, Y. Hassaine, S. Fliscounakis, L. Platbrood, M. Ortega-Vazquez, J. L. Martinez-Ramos, and L. Wehenkel, “Security management under uncertainty: From day-ahead planning to intraday operation,” in *VIII IREP Symposium on Bulk Power System Dynamics and Control (IREP)*, Buzios, Brazil, Aug 2010.
- [8] F. Capitanescu, S. Fliscounakis, P. Panciatici, and L. Wehenkel, “Cautious operation planning under uncertainties,” *IEEE Transactions on Power Systems*, vol. 27, no. 4, pp. 1859–1869, Nov 2012.
- [9] J. Warrington, P. J. Gouhart, S. Mariethoz, and M. Morari, “Policy-based reserves for power systems,” *IEEE Transactions on Power Systems*, vol. 28, no. 4, pp. 4427–4437, 2013.
- [10] A. Lorca, A. X. Sun, E. Litvinov, and T. Zheng, “Multistage adaptive robust optimization for the unit commitment problem,” to appear in *Operations Research*, 2015.
- [11] A. Lorca, “Robust Optimization for Renewable Energy Integration in Power System Operations,” dissertation, Georgia Institute of Technology, School of Industrial and Systems Engineering, Aug. 2016.
- [12] H. Zhang and P. Li, “Chance constrained programming for optimal power flow under uncertainty,” *IEEE Transactions on Power Systems*, vol. 26, no. 4, pp. 2417–2424, Nov 2011.
- [13] G. Li and X. P. Zhang, “Stochastic optimal power flow approach considering correlated probabilistic load and wind farm generation,” in *IET Conference on Reliability of Transmission and Distribution Networks (RTDN 2011)*, Nov 2011, pp. 1–7.
- [14] M. Vrakopoulou, K. Margellos, J. Lygeros, and G. Andersson, “Probabilistic guarantees for the N-1 security of systems with wind power generation,” in *Probabilistic Methods Applied to Power Systems (PMAPS) 2012*, Istanbul, Turkey, 2012.

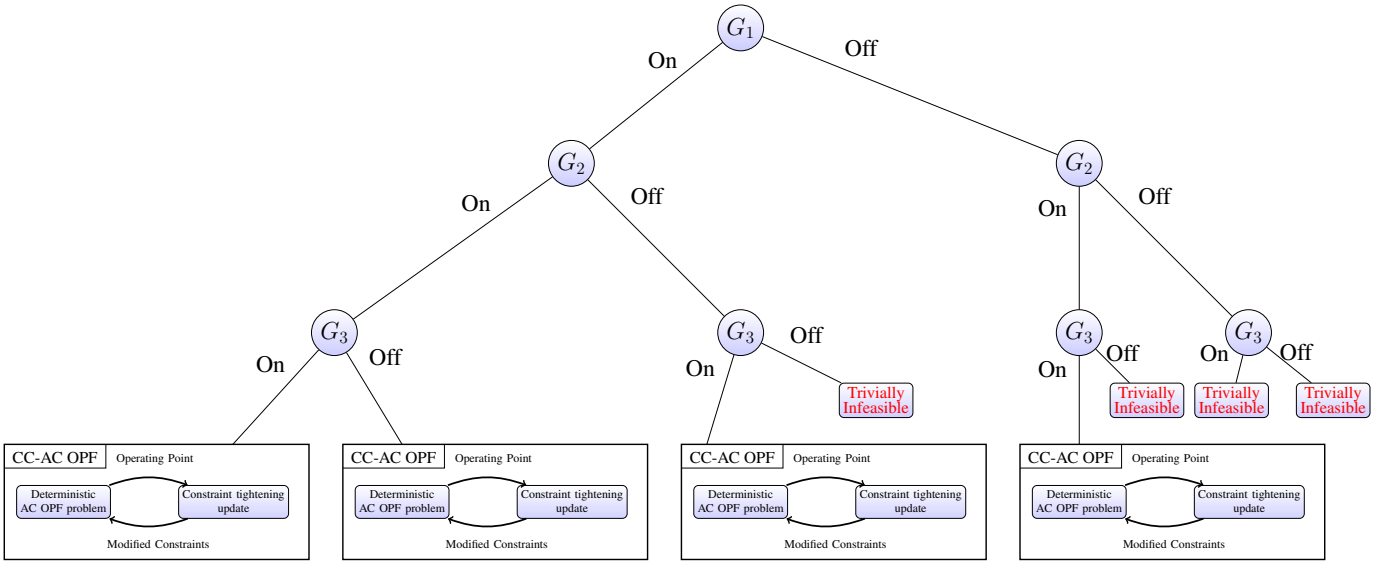


Fig. 13. Application of the alternate CC-AC UC approach to a modified version of the six-bus test case from [53]. Rather than iterate between solving a deterministic unit commitment problem and updating the constraint tightenings as shown in Fig. 6, the alternative approach solves multiple CC-AC OPF problems, each corresponding to a combination of the binary variables representing the generators' statuses. With total available generation less than the total load, the CC-AC OPF problems associated with certain combinations of the generators' statuses are trivially infeasible. The CC-AC OPF problems associated with other combinations may be feasible or infeasible depending on the constraint tightenings. See Fig. 14 for an illustration of this algorithm using the feasible space of the test case.

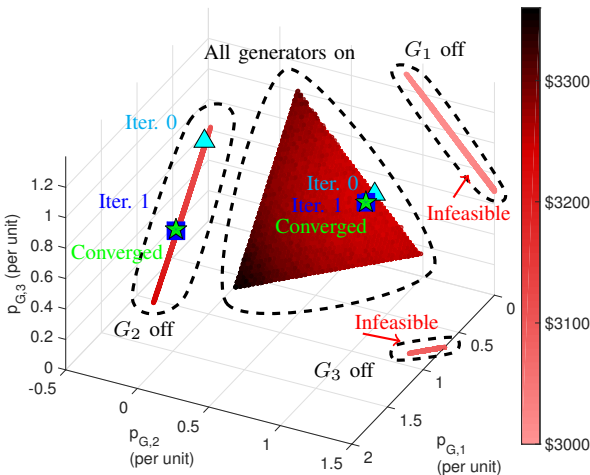


Fig. 14. Illustration of the alternate approach summarized in Fig. 13 using a modified version of the six-bus test case from [53]. This approach creates multiple CC-AC OPF problems corresponding to each combination of the generators' on/off statuses. This figure shows the feasible space associated with the deterministic AC OPF problem, where each region surrounded by a dashed black line corresponds to a different set of generator statuses (with the generator status listed next to the regions). Although the deterministic AC OPF problem would be feasible as long as any two generators are turned on, the tightening of the constraints make the CC-AC OPF problems corresponding to the cases with either generator 1 off or generator 3 off infeasible. For the case where all generators are on and the case where only generator 2 is off, the CC-AC OPF algorithm has iterations shown by the light-blue triangles (iteration 0) and the blue squares (iteration 1) in the respective regions of the feasible space. For each problem, CC-AC OPF algorithm converges to the points denoted by the green stars. The CC-AC OPF solution in the region for which generator 2 is off has the least cost and is therefore the solution to the alternate algorithm for the CC-AC UC problem.

- [15] M. Vrakopoulou, M. Katsampani, K. Margellos, J. Lygeros, and G. Andersson, "Probabilistic security-constrained AC optimal power flow," in *IEEE PowerTech Conference*, Grenoble, France, June 2013.
- [16] L. Roald, F. Oldewurtel, T. Krause, and G. Andersson, "Analytical reformulation of security constrained optimal power flow with probabilistic constraints," in *IEEE PowerTech Conference*, Grenoble, France, 2013.
- [17] D. Bienstock, M. Chertkov, and S. Harnett, "Chance-constrained optimal power flow: Risk-aware network control under uncertainty," *SIAM Review*, vol. 56, no. 3, pp. 461–495, 2014.
- [18] T. Summers, J. Warrington, M. Morari, and J. Lygeros, "Stochastic optimal power flow based on convex approximations of chance constraints," in *Power Systems Computation Conference (PSCC)*, Aug. 2014, pp. 1–7.
- [19] J. Schmidli, L. Roald, S. Chatzivasileiadis, and G. Andersson, "Stochastic AC optimal power flow with approximate chance-constraints," in *IEEE PES General Meeting*, Boston, 2016.
- [20] K. Baker, E. Dall'Anese, and T. Summers, "Distribution-agnostic stochastic optimal power flow for distribution grids," in *IEEE North American Power Symposium (NAPS)*, Denver, CO, 2016.
- [21] L. Roald, S. Misra, M. Chertkov, and G. Andersson, "Optimal power flow with weighted chance constraints and general policies for generation control," in *IEEE Conference on Decision and Control (CDC) 2015*, Osaka, Japan, 2015.
- [22] L. Roald, S. Misra, M. Chertkov, S. Backhaus, and G. Andersson, "Optimal power flow with wind power control and limited expected risk of overloads," in *Power System Computation Conference (PSCC) 2016*, Genova, Italy, 2016.
- [23] L. Roald and G. Andersson, "Chance-Constrained AC Optimal Power Flow: Reformulations and Efficient Algorithms," Jun. 2017. [Online]. Available: <https://arxiv.org/abs/1706.03241>
- [24] N. Amjady, S. Dehghan, A. Attarha, and A. J. Conejo, "Adaptive robust network-constrained AC unit commitment," *IEEE Transactions on Power Systems*, vol. 32, no. 1, pp. 672–683, Jan 2017.
- [25] A. Venzke, L. Halilbasic, U. Markovic, G. Hug, and S. Chatzivasileiadis, "Convex relaxations of chance constrained AC optimal power flow," 2017. [Online]. Available: <http://arxiv.org/abs/1702.08372>
- [26] H. Qu, L. Roald, and G. Andersson, "Uncertainty margins for probabilistic AC security assessment," in *IEEE PowerTech Conference*, Eindhoven, Netherlands, June 2015.
- [27] R. D. Zimmerman, C. E. Murillo-Sánchez, and R. J. Thomas, "MATPOWER: Steady-state operations, planning, and analysis tools for power

- systems research and education," *IEEE Transactions on Power Systems*, vol. 26, no. 1, pp. 12–19, 2011.
- [28] J. Carpentier, "Contribution to the economic dispatch problem," *Bulletin de la Societe Francaise des Electriciens*, vol. 8, no. 3, pp. 431–447, 1962.
- [29] J. A. Momoh, R. Adapa, and M. E. El-Hawary, "A review of selected optimal power flow literature to 1993. Parts I and II," *IEEE Transactions on Power Systems*, vol. 14, no. 1, pp. 96–111, Feb. 1999.
- [30] A. Castillo and R. P. O'Neill, "Survey of approaches to solving the ACOPF (OPF paper 4)," US Federal Energy Regulatory Commission, Tech. Rep., Mar. 2013.
- [31] F. Capitanescu, J. L. M. Ramos, P. Panciatici, D. Kirschen, A. M. Marcolini, L. Platbrood, and L. Wehenkel, "State-of-the-art, challenges, and future trends in security constrained optimal power flow," *Electric Power Systems Research*, vol. 81, no. 8, pp. 1731 – 1741, 2011.
- [32] J. Lavaei and S. H. Low, "Zero duality gap in optimal power flow problem," *IEEE Transactions on Power Systems*, vol. 27, no. 1, pp. 92–107, Feb. 2012.
- [33] S. H. Low, "Convex Relaxation of Optimal Power Flow—Parts I: Formulations and Equivalence," *IEEE Trans. Control Network Syst.*, vol. 1, no. 1, pp. 15–27, Mar. 2014.
- [34] C. Coffrin, H. L. Hijazi, and P. Van Hentenryck, "The QC relaxation: A theoretical and computational study on optimal power flow," *IEEE Transactions on Power Systems*, vol. 31, no. 4, pp. 3008–3018, July 2016.
- [35] D. K. Molzahn and I. A. Hiskens, "Sparsity-exploiting moment-based relaxations of the optimal power flow problem," *IEEE Transactions on Power Systems*, vol. 30, no. 6, pp. 3168–3180, Nov 2015.
- [36] C. Josz and D. K. Molzahn, "Moment/Sum-of-Squares Hierarchy for Complex Polynomial Optimization," *Submitted. Preprint available: http://arxiv.org/abs/1508.02068*, Aug. 2015.
- [37] B. Kocuk, S. S. Dey, and A. X. Sun, "Strong SOCP relaxations of the optimal power flow problem," *Operations Research*, vol. 64, no. 6, pp. 1177–1196, Nov.-Dec. 2016.
- [38] J. F. Marley, D. K. Molzahn, and I. A. Hiskens, "Solving multiperiod OPF problems using an AC-QP algorithm initialized with an SOCP relaxation," to appear in *IEEE Transactions on Power Systems*, 2017.
- [39] R. Madani, S. Sojoudi, and J. Lavaei, "Convex Relaxation for Optimal Power Flow Problem: Mesh Networks," *IEEE Trans. Power Syst.*, vol. 30, no. 1, pp. 199–211, Jan. 2015.
- [40] D. Wu, D. K. Molzahn, B. C. Lesieutre, and K. Dvijotham, "A Deterministic Method to Identify Multiple Local Extrema for the AC Optimal Power Flow Problem," to appear in *IEEE Trans. Power Syst.*, 2017.
- [41] M. Lubin, Y. Dvorkin, and S. Backhaus, "A robust approach to chance constrained optimal power flow with renewable generation," *IEEE Transactions on Power Systems*, vol. 31, no. 5, pp. 3840–3849, Sept. 2016.
- [42] L. Roald, F. Oldewurtel, B. Van Parys, and G. Andersson, "Security constrained optimal power flow with distributionally robust chance constraints," *Tech. Rep.*, 2015. [Online]. Available: <http://arxiv.org/abs/1508.06061>
- [43] P. Belotti, C. Kirches, S. Leyffer, J. Linderoth, J. Luedtke, and A. Mahajan, "Mixed-integer nonlinear optimization," *Acta Numerica*, vol. 22, pp. 1–131, 2013.
- [44] D. Bienstock and A. Verma, "Strong NP-hardness of AC power flows feasibility," *arXiv:1512.07315*, Dec. 2015.
- [45] I. Hiskens and R. Davy, "Exploring the power flow solution space boundary," *IEEE Transactions on Power Systems*, vol. 16, no. 3, pp. 389–395, 2001.
- [46] B. C. Lesieutre and I. A. Hiskens, "Convexity of the set of feasible injections and revenue adequacy in FTR markets," *IEEE Transactions on Power Systems*, vol. 20, no. 4, pp. 1790–1798, Nov. 2005.
- [47] B. Zhang and D. Tse, "Geometry of feasible injection region of power networks," in *49th Annual Allerton Conference on Communication, Control, and Computing*, Sept. 2011, pp. 1508–1515.
- [48] W. A. Bukhsh, A. Grothey, K. McKinnon, and P. A. Trodden, "Local solutions of the optimal power flow problem," *IEEE Transactions on Power Systems*, vol. 28, no. 4, pp. 4780–4788, 2013.
- [49] D. K. Molzahn, "Computing the feasible spaces of optimal power flow problems," to appear in *IEEE Transactions on Power Systems*, 2017.
- [50] E. M. B. Smith and C. C. Pantelides, "A symbolic reformulation/spatial branch-and-bound algorithm for the global optimisation of nonconvex MINLPs," *Computers & Chemical Engineering*, vol. 23, no. 4, pp. 457–478, 1999.
- [51] M. Tawarmalani and N. V. Sahinidis, "A polyhedral branch-and-cut approach to global optimization," *Mathematical Programming*, vol. 103, no. 2, pp. 225–249, 2005.
- [52] H. Nagarajan, M. Lu, E. Yamangil, and R. Bent, "Tightening McCormick relaxations for nonlinear programs via dynamic multivariate partitioning," *arXiv:1606.05806*.
- [53] A. J. Wood and B. F. Wollenberg, *Power Generation, Operation, and Control*. John Wiley & Sons, 2012.